Fabrication of antibacterial PVA/Bentonite/Ag Composite Nanofibers with Bio-AgNPs synthesized with *Fusarium sporotrichioides*

Zahra Beagom Mokhtari-Hooseini (z.mokhtari@hsu.ac.ir)
Hakim Sabzevari University
Ashrafalsadat Hatamian-Zarmi
University of Tehran, Tehran
Soheila Mahdizadeh
University of Tehran, Tehran
Bahman Ebrahimi-Hosseinzadeh
University of Tehran, Tehran
Hale Alvandi
University of Tehran, Tehran

Research Article

Keywords: Fusarium sporotrichioides, Silver nanoparticles, Composite nanofiber, Bentonite, Polyvinylalcohol (PVA)

Posted Date: January 24th, 2022

DOI: https://doi.org/10.21203/rs.3.rs-1273852/v1

Abstract

Nowadays, membranes and filters made of nanofibers are extensively considered in various fields, such as medicine, water purification, etc. Using an environmentally-friendly method, this study fabricated a nanofiber-based on PVA, bentonite, and silver nanoparticles (AgNPs) with good mechanical strength. Due to conventional AgNPs synthesis methods' toxicity, AgNPs were synthesized by *Fusarium sporotrichioides*. The MGYP culture medium and the $AgNO_3$ 12 M were optimal for Bio-AgNPs synthesis. Bio-AgNPs particle size and zeta potentials were 58 nm and -16.8 mV, respectively. The growth inhibition zone of Bio-AgNPs in *E. coli* and *S. aureus* was 0.53 and 0.80 mm, respectively and comparable with chloramphenicol. Then, the optimized Bio-AgNPs and a sample with chemical synthesis AgNPs were used to prepare the PVA/nano-Bentonite/nano-Ag (PVA/NB/AgNPs) nanofiber. The presence of silver in the nanofibers was confirmed through EDX and XRD methods. The diameter of nanofibers was 230 nm. The antibacterial activity of PVA/NB/Bio-AgNPs nanofibers was significantly better against both gram-positive and gram-negative bacteria compared to PVA/NB/Chem-AgNPs nanofibers. The produced membrane is suitable for water treatment, food packaging, and wound dressing because of its good thermal, mechanical, and antibacterial properties.

1. Introduction

The first use of nanosilver particles was reported in 1800. Moreover, they were used in 1954 in swimming pools and in 1970 for filtering (treating) drinking water. Nanosilver particles have a wide range of strong antibacterial activity. Nowadays, nanosilver particles are used for the disinfection of various systems and as bio-anti-fouling [1]. Ag nanoparticles (AgNPs) are used in antibacterial filters, water disinfection, wound dressing, sensors, chemical gas filtration, protective fabrics, and air purifiers, among others [2, 3]. There are several hypotheses for the mechanism behind the effect of AgNPs on the cells. One hypothesis involves the attachment of AgNPs to the cell membrane, leading to a reduction in lipopolysaccharide molecules and the formation of a hole on the cell’s surface, which will increase the permeability of the cell membrane. Another hypothesis posits that AgNPs go into the cell and damage the DNA, while another involves the dissolution of AgNPs and the release of Ag+ ions that have an antibacterial property [4, 5].

Chemical methods for AgNPs synthesis are unreliable. For example, some toxic compounds, such as sodium borate, are used in the chemical synthesis that are dangerous and pollute the environment. Therefore, the biosynthesis of nanoparticles using microorganisms is a new promising way to overcome these problems [6, 7]. In this method, intracellular or extracellular enzymes produce Ag^0 from Ag^+ [8]. For the industrial biosynthesis of AgNPs, a microorganism must be found with a high ability for the synthesis of nanoparticles, while having saprophytic and pathogenic properties.

Several studies have been conducted on nanosilver biosynthesis using different microorganisms, such as *Aspergillus* spp., *Fusarium* spp., *Bacillus* spp., *Caralluma* spp., and recombinant *Escherichia coli*, and so on [9–12]. However, none of these methods have yet been utilized at an industrial scale. Microorganisms that produce extracellular enzymes are more favorable for the production of AgNPs because they reduce

the level of downstream processing. Among these microorganisms, fungi are more suitable because their purification process is simpler. In addition, according to published reports, fungi are better than bacteria in terms of the secretion amount of proteins and enzymes. Many enzymes secreted by fungi are capable of reducing metal ions through environmentally-friendly processes. Fungi can synthesize different types of metal nanoparticles, such as nanosilver and nanogold [13]. The mechanism for producing nanoparticles using fungal microorganisms is not entirely clear. One reported mechanism suggests a reduction of Ag^{+} to Ag^{0} due to a conjugation between the electron shuttles and the NADH-dependent reductase. The actual reduction mechanism may be due to the transfer of an electron from NADH, while the NADH-dependent enzyme acts as an electron carrier [8, 14, 15].

AgNPs have antifungal, antibacterial, and antivirus activity. They suppress inflammation and have anti-platelet and anti-angiogenesis activity. AgNPs are used in many fields, such as medicine (e.g., burn treatment and production of dental materials), water treatment, and disinfection. One application of nanosilver involves adding them into the structure of membranes and nanofibers to increase their antibacterial properties [16–18].

Electrospinning is a relatively simple method for nanofiber production, which can be attractive for medical engineering, filtration, protective clothing production, catalytic reactions, and sensors [19–21]. In the electrospinning process, a high voltage is applied to create charged electric jets from the polymer solution. The resulting nanofibers form on a collecting plate. The electrospinning technique is highly adaptable and produces a wide range of polymer materials with different fiber diameters (ranging from nanometers to micrometers). Moreover, different types of molecules can easily be involved in the process of producing functional nanofibers [22]. Factors affecting the thickness and the morphology of nanofibers include molecular weight, the distribution of the molecular weight and the morphology of the polymer (branching, linear), the solution's properties (viscosity, conductivity, and surface tension), process parameters (electrical potential, flow rate, the distance between the polymer solution and the collector), and environmental parameters (temperature, humidity, and air velocity in the electrospinning chamber) [23]. The size and morphology of nanofibers can be controlled using these different operational variables.

Small pores size, high permeability, low weight, and high surface to volume ratio are some of the advantages of electrospinning nanofibers. These properties have resulted in using electrospinning nanofibers in various fields. For instance, they can be used for the production of membranes for the antimicrobial treatment of water instead of conventional water treatment methods because of the above-mentioned properties [24]. Moreover, they are a good candidate for producing wound dressing [25].

Many studies have been conducted on improving the properties of the produced nanofiber, e.g., improving mechanical and thermal properties by adding a filler to the polymer. Some researchers have been interested in creating composite polymers using minerals. One of these minerals is bentonite. The reason for considering this mineral as a polymer filler is that adding a low amount of it can improve the mechanical and thermal properties, while making the produced nanocomposite nonflammable [26–28]. Our previous study, focusing on the production, optimization, and characterization of PVA/nano-bentonite

composite nanofibers, has shown that adding nano-bentonite (NB) to PVA improves the mechanical and thermal properties of PVA nanofibers [29].

The main objectives of the current study include the green synthesis of nanosilver particles using *Fusarium sporotrichioides*, optimizing the production process using the one-factor-at-a-time method, characterizing the produced nanosilver, loading it on the PVA/NB nanofiber, and studying the produced nanocomposite.

2. Materials And Methods

All the materials and the culture medium used in this study were purchased from reputable companies with a laboratory grade.

2.1. Biosynthesis of AgNPs

2.1.1. The Preparation and Maintenance of the Fungi

F. sporotrichioides was obtained from the Iranian Biological Resources Center, it was cultured on potato dextrose agar (PDA) at 30°C for 5 days, and it was then maintained at 4°C.

2.1.2. AgNPs Production

To prepare the inoculum, a 5-mm disk of mycelial solid culture was transferred into the selected medium and incubated at 28 °C and 150 rpm for 7 days. In order to produce AgNPs, *F. sporotrichioides* was cultured in a liquid medium with 1% v/v of inoculum at 28°C and 150 rpm of shaking for 48 h. Then, the biomass was separated from the fermentation broth using a filter under sterile conditions. Afterward, 30 ml of the $AgNO_3$ solution with the selected concentration was added to 100 ml of supernatant, followed by incubation at 28°C and 150 rpm for 24h under dark conditions. Then, the produced nanoparticles were separated using centrifugation at 10000 rpm for 10 min. Finally, the sediment nanoparticles were rinsed three times with distilled water.

2.1.3. The Optimization of the Process

The suitable conditions of two factors were determined using the one-factor-at-a-time method. The type of culture medium and the concentration of $AgNO_3$ were studied. At first, two liquid media, i.e., PDB (potato dextrose broth) and MGYP (malt extract, glucose, yeast extract, and peptone), were investigated in terms of the quality and quantity of AgNPs production under culture conditions of 28°C and 150 rpm for 48h. Then, the concentration of $AgNO_3$ in the selected medium was determined.

2.2. Characterization of AgNPs

Primary verification of AgNPs biosynthesis: Macroscopic observation and UV-visible spectra were used for verifying the biosynthesis of AgNPs.

Size and Surface Charge: Dynamic Light Scattering (DLS) (Zetasizer Nano ZS, Malvern Co.) was used for evaluating the size and the surface charge of the produced AgNPs seven days after AgNPs production. The average size of the particles was obtained using the measured data. Moreover, the surface charge of the particles was measured as the zeta potential based on the rate of movement of the particles toward the electrodes and the electrical and kinetic energies of the particles [16, 30].

Morphology: The morphology of the synthesized AgNPs was evaluated using Field Emission Scanning Electron Microscope (FE-SEM). To do so, after separating nanoparticles using centrifugation, the sediment was rinsed and dried. A thin layer of Au was dispersed on the dried nanoparticles using DS-sputtering at relative vacuum and 24 mA. The Au-covered nanoparticles were placed in FE-SEM, and the image of the nanoparticles was taken at the selected scales and at a voltage of 15 kV.

Antibacterial activity: The antibacterial activity of the biosynthesized AgNPs (Bio-AgNPs) and the purchased AgNPs synthesized using the chemical method (Chem-AgNPs) was investigated using the disk diffusion approach according to our previous study [31]. *Staphylococcus aureus* (UTMC 1429) and *Escherichia coli* (PTCC 126) were used as representatives of gram-positive and gram-negative bacteria, respectively [32]. Sterile disks were placed inside AgNPs solution with three concentrations (3, 6, 12 mM) for 24 h. After culturing the bacteria in a nutrient agar medium, the discs were placed in the medium, and the antibacterial activity was evaluated after 24 hours [31]. 0.5 McFarland solution of each bacterium was used as a negative control [33]. A common antibiotic, i.e., chloramphenicol, was used as the standard control sample.

2.3. Production of PVA/NB/AgNPs

2.3.1. Preparation of PVA/NB Membrane

The washed NB produced by the ball mill was added to distilled water and mixed using a magnetic stirrer for one hour. Then, the 7.5% w/w PVA solution was added to the NB solution and mixed with a stirrer at 80°C for 2h until a uniform suspension was obtained. The nanofiber was produced by electrospinning the prepared solution using a high-voltage power supply electrospinning device (Fanavaran Nano-Meghyas, Model: ES1000, Iran). The operation conditions included a voltage of 11 kV, a feeding rate of 0.5 mL/h, a 15-cm distance between the needle and the collector, and a bentonite concentration of 3% w/w, optimized in the previous research study [29].

2.3.2. Preparation of PVA/NB/AgNPs Membrane

After the suspension of NB in distilled water and mixing it for one hour, the 7.5% PVA solution was added and mixed for 2h at 80°C. The mixture was cooled to ambient temperature, and, then, the suspension of AgNPs (5% w/w in the composite nanofiber) was added to the mixture and mixed for 2h until a uniform suspension was obtained. The composite nanofiber was produced from this suspension through electrospinning according to the above conditions.

The fibers were collected on an electrically-grounded aluminum foil placed 15 cm from the needle tip. The PVA/NB/AgNPs nanofibers were cross-linked in glutaraldehyde and HCl vapor at 80 ºC for 1 h. Then, the glutaraldehyde that had not reacted was removed by 10% glycine solution.

2.4. Characterization of PVA/NB/AgNPs

Morphology: The diameter and morphological properties of the produced nanofiber were studied by SEM after covering it with an Au layer. The diameter of the nanofibers and their morphology were specified using Field Emission Scanning Electron Microscopy (FE-SEM, S4160, Hitachi, Japan). The mean diameter of the nanofibers was specified by the ImageJ software.

The Chemical Characterization of the Nanofiber: The presence of Ag and bentonite in the produced composite nanofiber was verified using Energy-Dispersive Spectroscopy (EDX). The structure and the functional group of the produced nanofibers were investigated using Fourier transform infrared spectroscopy (FTIR). Moreover, X-Ray Diffraction (XRD) was used for verifying the presence of NB and Ag in the nanofiber.

Antibacterial activity: The antibacterial activity of the PVA/NB/Bio-AgNPs and PVA/NB/Chem-AgNPs membrane was investigated using the disk diffusion approach same as pervious step.

3. Results And Discussion

3.1. AgNPs Biosynthesis

The production of nanoparticles was verified using two simple methods. The simplest way for verifying the production of nano-Ag involves macroscopic observation, i.e., a change of color in the liquid process from yellow to brown [34]. Figure 1(a) indicates the liquid reaction before and after the process, showing the change in color from yellow to brown. The other method for the primary verification of AgNPs biosynthesis is determining the maximum absorption of the processed liquid. If the processing liquid has the maximum absorption at around 420 nm, the nano-Ag has been produced. Figure 1(b) shows that the maximum absorption of the reaction solution is at 420 nm, verifying the formation of AgNPs.

Figure 1 *near here*

3.2. The Optimization of Parameters Influencing the Process

In general, two factors affect AgNPs production bioprocesses, i.e., the type of culture medium and the concentration of $AgNO_3$. The one-factor-at-a-time method was used for determining the optimum conditions.

Media selection: Two common media for growing fungi, i.e., PDB and MGYP, were investigated for AgNPs production. *F. sporotrichioides* was separately cultured in each medium with 10% v/v inoculum, followed

by incubation for 48h at 28°C and 150 rpm. The supernatant (i.e., the fermentation broth) was separated from the biomass, and it was used for AgNPs production. Accordingly, 100 ml of the supernatant was added to 100 ml of the $AgNO_3$ solution (C=3mM), followed by incubation under dark conditions at 28°C and 150 rpm for 24 h. The change in the color from yellow to brown indicates the reduction of Ag and the production of nano-Ag. The observation of λ_{max} at sizes higher than 400 nm verifies the formation of the nanoparticles. In both media, nano-Ag was synthesized. The λ_{max} was observed at 410 and 420 nm in PDB and MGYP media, respectively. The size of the nanoparticles and the zeta potential were measured for both media using DLS. The average diameters and the zeta potential of the nanoparticles produced using the fermentation broth of the PDB medium were 16 nm and (-6.50 mV), while they were 13 nm and (-15.9 mV) for the MGYP medium, respectively. The higher the absolute value of the zeta potential, the more stable the particle. According to these results, the AgNPs produced in MGYP are more stable and desirable. This can be explained based on the compositions of the media. In MGYP, the source of carbon is a monosaccharide, while the carbon source in PDB is a polysaccharide; hence, the reductase enzyme in the supernatant of MGYP is higher than in PDB. Therefore, MGYP was selected for the rest of the analyses.

The Concentration of $AgNO_3$: Three concentrations of $AgNO_3$, i.e., 3, 6, and 12 mM, were studied for the production of AgNPs in the MGYP medium according to the above conditions. The λ_{max} of 3 and 6 mM is 420 nm, while it is 430 nm for 12mM. The amount of adsorption in λ_{max} increased by increasing the concentration of the $AgNO_3$ solution. The size and the zeta potential of the biosynthesized nano-Ag were measured. Figure 5 shows the size of AgNPs in three concentrations of $AgNO_3$. The average diameter of AgNPs is 13, 79, and 58 nm in 3, 6, and 12 mM of $AgNO_3$, respectively. The standard deviation of the diameter of the nanoparticles for 3 and 6 mM are similar; however, they are higher in 12 mM. The zeta potential of the produced nanoparticles was determined (Figure 2). The zeta potential is (-15.9), (-16.9), and (-16.1) for 3, 6, and 12 mM, respectively. The zeta potential values of the three concentrations are close. Comparing the size of the produced nano-Ag indicates that the 3-mM concentration of $AgNO_3$ is the best concentration because the diameter is 13 nm, which is much smaller than the size in the two other concentrations, while the zeta potential values of the three concentrations are close.

Figure 2 *near here*

Based on the fact that AgNPs are usually used in membranes due to their antibacterial properties, AgNPs with a higher antibacterial activity were selected for loading on the membrane.

Then, *F. sporotrichioides* was cultured in the MGYP medium at 28°C and 150 rpm for 48 h. Afterward, an equal volume of fermentation broth was mixed with 12mM of the $AgNO_3$ solution, followed by incubation at 28°C and 150 rpm for 24 h. Bio-AgNPs were separated using centrifugation, and they were dried for next analyses.

The results of the extracellular biosynthesis of AgNPs using the fungi in other reports are similar to the findings of the present study. For example, Basavaraja et al. [35] produced AgNPs using *F. semitectum*

with a size of 10-60 nm, and Ingle et al. [36] produced AgNPs using *Fusarium solani* with a size of 5-35 nm.

3.3. Characterization of Produced AgNPs

The morphology of the produced nanoparticles was studied using Field Emission Scanning Electron Microscope (FE-SEM) at 1, 2 μm, 500, and 200nm scale. According to Figure 3, the nanoparticle has a regular sphere shape with smooth surface. The size of nanoparticles was between 10 and 80 nm.

Figure 3 *near here*

The synthesized nanoparticles were investigated by FTIR (Figure 4). The peak of 3457 cm^{-1} indicates the O-H functional group. This functional group is probably related to the water that had attached to AgNPs. Two peaks at 1398 cm^{-1} and 1633 cm^{-1} are observed, showing the amid groups of proteins and reduction enzymes, which verify the biosynthesis of AgNPs [37, 38]. This peak can be related to the Ag-O band. Harish Kumar believes that the peak of the metal oxide was observed in this range [39]. Chen et al. (2016) observed that in the mycosynthesis of AgNPs with *Cordyceps sinensis*, the AgNPs bind to O-H groups on the polysaccharide [40].

Figure 4 *near here*

The antibacterial activity of Bio-AgNPs and chem-AgNPs was investigated using disk diffusion (Figure 5). This figure shows the antibacterial effect of Bio-AgNPs at different $AgNO_3$ concentrations for both positive and negative-gram bacteria. According to the results, as the concentration of $AgNO_3$ increased, the antibacterial property against both types of bacteria increased as well. AgNPs with a concentration of 12 mM and a size of 58 nm had the highest antibacterial properties against *E. coli* and *S. aureus*. This can be explained based on the size of the produced AgNPs. AgNPs with a smaller diameter can pass through the cell membrane, so they are absorbed by vacuoles and cannot affect the cell's metabolism. The larger AgNPs cannot easily pass through the cell membrane; hence, they have a lower effect on the cell growth. The medium size is the most effective for the inhibition of cell growth. Regarding the size of AgNPs at different concentrations of $AgNO_3$, the middle size is obtained by the highest concentration. The growth inhibition zone of these nanoparticles in *E. coli* and *S. aureus* was 0.53 and 0.80 mm, respectively. This inhibitory zone was comparable to chlorphenicol (0.66 mm). The exact antibacterial mechanism of AgNPs is unknown, but it seems they interact with the sulfhydryl group of proteins and DNA bases to inhibit respiration and replication in bacteria [41–44]. The antibacterial effect of Bio-AgNPs against *S. aureus* and *E. coli* was higher than that of Chem-AgNPs. This effect could be due to the greater stability of Bio-AgNPs than Chem-AgNPs [45]. In all the samples, the antibacterial effect on *E. coli* was higher than the effect on *S. aureus*.

Figure 5 *near here*

3.4. PVA/NB/AgNPs Production

According to the previous study, PVA/NB has good thermal and mechanical properties [29]. Therefore, the produced AgNPs were used for the production of the PVA/NB/AgNPs composite nanofiber in order to improve the antibacterial activity of the PVA/NB nanofiber. PVA/NB/AgNPs nanofibers were produced using electrospinning with Bio-AgNPs and Chem-AgNPs.

Characterization of PVA/NB/AgNPs

The PVA/NB spectra loaded with AgNPs synthesized from the fungus are similar to the crosslink nanofiber spectrum but the peak intensities were reduced (Figure 6). This decrease is due to the combination of AgNPs with PVA/NB. Also, the links created between PVA/NB/AgNPs with glutaraldehyde. The peak in 2886 cm^{-1} was related to grafting H-C aldehyde. Crosslinking PVA with glutaraldehyde shortened the O-H peak (3392 cm^{-1}) compared to PVA/NB [46]. This observation suggests that hydrogen bonds become weaker in the cross-link state. According to the figure, no difference was observed between the spectra of nanofibers loaded with Chem-AgNPs.

Figure 6 *near here*

Bio-AgNPs and Chem-AgNPs were separately loaded onto the PVA/NB nanofibers. The produced nanofibers were investigated using FESEM (Figure 7), and the porosity, the average diameter, and the standard deviation of the diameter of the nanofibers were determined by the imaging software. The average diameter of the nanofibers for both AgNPs was 230 nm, while the standard deviation of the nanofibers with Bio-AgNPs (0.055) was lower than that of the nanofiber with Chem-AgNPs (0.073). The porosity of the nanofiber loaded with Bio-AgNPs was 0.478, which was higher than that of the nanofiber loaded with Chem-AgNPs with a porosity of 0.371.

To verify the loading of AgNPs on the PVA/NB nanofibers and to show the dispersion of AgNPs on the nanofibers, EDX was conducted. According to the EDX results in Figure 7, AgNPs were loaded on the nanofibers with good dispersion.

Figure 7 *near here*

The produced nanofibers were studied using XRD, and the presence of Ag was verified. XRD was conducted for PVA, NB, PVA/NB, and both PVA/NB/AgNPs (Figure 8). After electrospinning NB with PVA, the crystalline state of NB was not observed. The two peaks, i.e., $2\theta = 38$ and $2\theta = 44$, in the XRD results are related to Ag in the produced nanofibers. These peaks are observed in the XRD patterns of the pure crystalline Ag [47].

Figure 8 *near here*

Examination of the antibacterial properties of PVA/NB/AgNPs nanofibers using the disk diffusion method shows that both samples, i.e., Bio-AgNPs and Chem-AgNPs, are more sensitive to gram-negative bacteria than the gram-positive ones. Moreover, this test indicates that the antibacterial effect of PVA/NB nanofibers loaded with Bio-AgNPs is significantly higher ($p<0.05$) than that of the nanofibers loaded with

Chem-AgNPs (Table 1). PVA/NB/AgNPs nanofibers with stability and strength of structure can be used for various applications. These PVA/NB/AgNPs nanofibers can trap bacteria. The presence of AgNPs in this structure with antibacterial activity by various mechanisms kills bacteria and prevents the formation of biofilms. One of the significant advantages of AgNPs compared to antibiotics is that no bacterial resistance has been reported [41, 48–50]. Therefore, one of the most important uses of this structure can be in water purification and food packaging.

Table 1
Inhibition zone of different samples against *E. coli* and *S. aureus*.

	E. coli (mm)	*S. aureus* (mm)
PVA/NB	0.05	0.03
PVA/NB/Chem-AgNPs	0.32	0.20
PVA/NB/Bio-AgNPs	0.62	0.36
Chloramphenicol	0.70	0.52

4. Conclusion

In this study, AgNPs were biosynthesized using *F. sporotrichioides*, and the biosynthesis process was optimized. According to the observations, the culture medium and the $AgNO_3$ concentration affect the product. The MGYP medium produced more stable AgNPs than the PDB medium. Changing $AgNO_3$ concentration did not have a significant effect on the stability of NPs; however, it affected the size and the antibacterial property of the NPs. The best antibacterial properties were obtained at the 12-mM concentration of $AgNO_3$ with AgNPs with a size of 58 nm. The good antibacterial properties of the biosynthesized AgNPs resulted in the antibacterial properties of PVA/NB nanofibers containing these bio-AgNPs. Therefore, the produced PVA/NB/Bio-AgNPs can be used in food packaging, wound dressing, and water treatment due to their good thermal, mechanical, and antibacterial properties.

Declarations

Acknowledgements

The authors would like to thank all people, who helped us during the experimental work.

Declaration of interests

The authors declare that they have no known competing financial interests or personal relationships that could have appeared to influence the work reported in this paper.

References

1. I. Gehrke, A. Geiser, A. Somborn-Schulz, Innovations in nanotechnology for water treatment. Nanotechnol Sci Appl. **8**, 1–17 (2015)
2. M. Botes, T. Eugene, Cloete, Crit. Rev. Microbiol. **36**, 1:68–81 (2010)
3. A. Shyam, S. Chandran, S.B. George, and S. E, Inorganic and Nano-Metal Chemistry **51**, 12:1646–1662 (2021)
4. S.A. Kumar, M.K. Abyaneh, S. Gosavi, S.K. Kulkarni, R. Pasricha, A. Ahmad, M. Khan, Biotechnol. Lett. **29**, 3:439–445 (2007)
5. P. Mukherjee, A. Ahmad, D. Mandal, S. Senapati, S.R. Sainkar, M.I. Khan, R. Ramani, R. Parischa, P. Ajayakumar, M. Alam, Angew. Chem. Int. Ed. **40**, 19:3585–3588 (2001)
6. S. Honary, K. Ghajar, P. Khazaeli, P. Shalchian, Tropical Journal of Pharmaceutical Research **10**, 1 (2011)
7. C. Nirmala, M. Sridevi, Journal of Inorganic and Organometallic Polymers and Materials. **31**, 9:3711–3725 (2021)
8. A. Ingle, A. Gade, S. Pierrat, C. Sonnichsen, M. Rai, Current Nanoscience **4**, 2:141–144 (2008)
9. P. Phanjom, G. Ahmed, Advances in Natural Sciences: Nanoscience and Nanotechnology. 8, 4:045016 (2017)
10. Q. Yuan, M. Bomma, Z. Xiao, Materials. **12**, 24:4180 (2019)
11. T. Yurtluk, F.A. Akçay, A. Avcı, Prep. Biochem. Biotechnol. **48**, 2:151–159 (2018)
12. Z. Zarei, D. Razmjoue, J. Karimi, J. Inorg. Organomet. Polym Mater. **30**, 11:4606–4614 (2020)
13. N. Krumov, I. Perner-Nochta, S. Oder, V. Gotcheva, A. Angelov, C. Posten, Chemical Engineering & Technology: Industrial Chemistry-Plant Equipment-Process Engineering-Biotechnology **32**, 7:1026–1035 (2009)
14. A. Rohaizad, S. Shahabuddin, M.M. Shahid, N.M. Rashid, Z.A.M. Hir, M.M. Ramly, K. Awang, C.W. Siong, Z. Aspanut, Journal of Environmental Chemical Engineering **8**, 4:103955 (2020)
15. M. Azadi, S. Siavash Moghaddam, A. Rahimi, L. Pourakbar, J. Popović-Djordjević, Journal of Environmental Chemical Engineering. **9**, 5:105919 (2021)
16. K. Kalishwaralal, V. Deepak, S.R.K. Pandian, M. Kottaisamy, S. BarathManiKanth, B. Kartikeyan, S. Gurunathan, Colloids and surfaces B: Biointerfaces. **77**, 2:257–262 (2010)
17. R.R. Palem, N. Saha, G.D. Shimoga, Z. Kronekova, M. Sláviková, P. Saha, International Journal of Polymeric Materials and Polymeric Biomaterials **67**, 1:1–10 (2018)
18. C. Boztepe, E. Tosun, T. Bilenler, K. Sislioglu, International Journal of Polymeric Materials and Polymeric Biomaterials. **66**, 18:934–942 (2017)
19. A. Bazargan, M. Keyanpour-Rad, F. Hesari, M.E. Ganji, Desalination. **265**(1-3), 148–152 (2011)
20. Z.-M. Huang, Y.-Z. Zhang, M. Kotaki, S. Ramakrishna, Compos. Sci. Technol. **63**, 15:2223–2253 (2003)
21. K. Tan, S.K. Obendorf, J. Membr. Sci. **305**(1-2), 287–298 (2007)

22. V. Beachley, X. Wen, Progress in polymer science. **35**, 7:868–892 (2010)
23. A. Haider, S. Haider, I.-K. Kang, Arabian Journal of Chemistry **11**, 8:1165–1188 (2018)
24. H. Chen, M. Huang, Y. Liu, L. Meng, M. Ma, Science of The Total Environment. **739**, 139944 (2020)
25. A. Memic, T. Abudula, H.S. Mohammed, K. Joshi Navare, T. Colombani, S.A. Bencherif, ACS Applied Bio Materials **2**, 3:952–969 (2019)
26. C.-N.H. Thuc, A.-C. Grillet, L. Reinert, F. Ohashi, H.H. Thuc, L. Duclaux, Appl. Clay Sci. **49**, 3:229–238 (2010)
27. H.W. Lee, M.R. Karim, H.M. Ji, J.H. Choi, H.D. Ghim, S.M. Park, W. Oh, J.H. Yeum, J. Appl. Polym. Sci. **113**, 3:1860–1867 (2009)
28. L. Gong, Y. Kong, H. Wu, Y. Ge, Z. Li, J. Inorg. Organomet. Polym Mater. **31**, 2:659–673 (2021)
29. S. Mahdizadeh, Z.-B. Mokhtari-Hosseini, A. Hatamian-Zarmi, B. Ebrahimi-Hosseinzadeh, Journal of Applied Research of Chemical-Polymer Engineering **2**, 2:17–28 (2018)
30. İA. Kariper, Journal of Inorganic and Organometallic Polymers and Materials. (2022)
31. N. Yasrebi, A.S. Hatamian Zarmi, M. Larypoor, Iranian Journal of Medical Microbiology **14**, 3:186–200 (2020)
32. H. Alvandi, A. Hatamian-Zarmi, B. Ebrahimi Hosseinzadeh, Z.-B. Mokhtari-Hosseini, Iranian Journal of Medical Microbiology **14**, 6:596–611 (2020)
33. H. Alvandi, A. Hatamian-Zarmi, B.E. Hosseinzadeh, Z.B. Mokhtari-Hosseini, E. Langer, H. Aghajani, Carbohydrate Polymer Technologies and Applications. **2**, 100159 (2021)
34. M.R. Safaee-Ardakani, A. Hatamian-Zarmi, S.M. Sadat, Z.B. Mokhtari-Hosseini, B. Ebrahimi-Hosseinzadeh, H. Kooshki, J. Rashidiani, Fibers Polym. **20**, 12:2493–2502 (2019)
35. S. Basavaraja, S. Balaji, A. Lagashetty, A. Rajasab, A. Venkataraman, Mater. Res. Bull. **43**, 5:1164–1170 (2008)
36. A. Ingle, M. Rai, A. Gade, M. Bawaskar, J. Nanopart. Res. **11**, 8:2079–2085 (2009)
37. S. Umoren, I. Obot, Z. Gasem, J. Mater. Environ. Sci. **5**, 3:907–914 (2014)
38. G.P. Chuy, P.C.L. Muraro, A.R. Viana, G. Pavoski, D.C.R. Espinosa, B.S. Vizzotto, W.L. da Silva, Journal of Inorganic and Organometallic Polymers and Materials. (2021)
39. H. Kumar, R. Rani, Int J Eng Innov Technol **3**, 3:344–348 (2013)
40. X. Chen, J.-K. Yan, J.-Y. Wu, Food Hydrocolloids **53**, 69–74 (2016)
41. M.N. Owaid, I.J. Ibraheem, European Journal of Nanomedicine. **9**, 1:5–23 (2017)
42. N. Shahabadi, S. Zendehcheshm, F. Khademi, K. Rashidi, K. Chehri, Journal of Environmental Chemical Engineering. **9**, 3:105215 (2021)
43. U. Latif, K. Al-Rubeaan, A.T. Saeb, International Journal of Polymeric Materials and Polymeric Biomaterials. **64**, 9:448–458 (2015)
44. S. Vijayakumar, M. Divya, B. Vaseeharan, J. Chen, M. Biruntha, L.P. Silva, E.F. Durán-Lara, K. Shreema, S. Ranjan, N. Dasgupta, J. Inorg. Organomet. Polym Mater. **31**, 2:624–635 (2021)

45. A. Irshad, N. Sarwar, H. Sadia, K. Malik, I. Javed, A. Irshad, M. Afzal, M. Abbas, H. Rizvi, International journal of biological macromolecules. **145**, 189–196 (2020)
46. E.F.d. Reis, F.S. Campos, A.P. Lage, R.C. Leite, L.G. Heneine, W.L. Vasconcelos, Z.I.P. Lobato, H.S. Mansur, Materials Research **9**, 2:185–191 (2006)
47. G.Z.S. Oliveira, C.A.P. Lopes, M.H. Sousa, L.P. Silva, International Nano Letters **9**, 2:109–117 (2019)
48. A. Ounkaew, N. Janaum, P. Kasemsiri, M. Okhawilai, S. Hiziroglu, P. Chindaprasirt, Journal of Environmental Chemical Engineering. **9**, 6:106793 (2021)
49. S. Iravani, Inorganic and Nano-Metal Chemistry. 51, 12:1615-1645 (2021)
50. S. Abdelkrim, A. Mokhtar, A. Djelad, F. Bennabi, A. Souna, A. Bengueddach, M. Sassi, J. Inorg. Organomet. Polym Mater. **30**, 3:831–840 (2020)

Figures

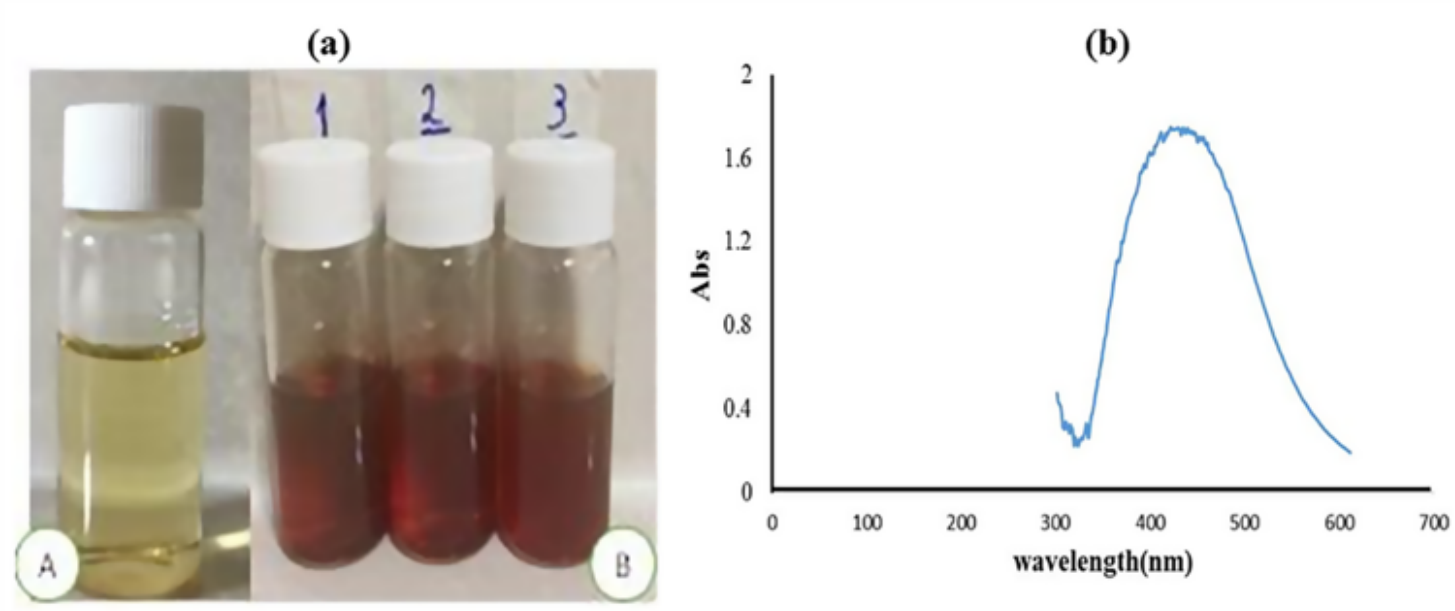

Figure 1

(a) Color changing in the biomass free of the fungal culture medium (MGYP) before the reaction (A) and after the reaction in different $AgNO_3$ concentrations (B); (b) The maximum absorption of the reaction solution after the AgNPs production.

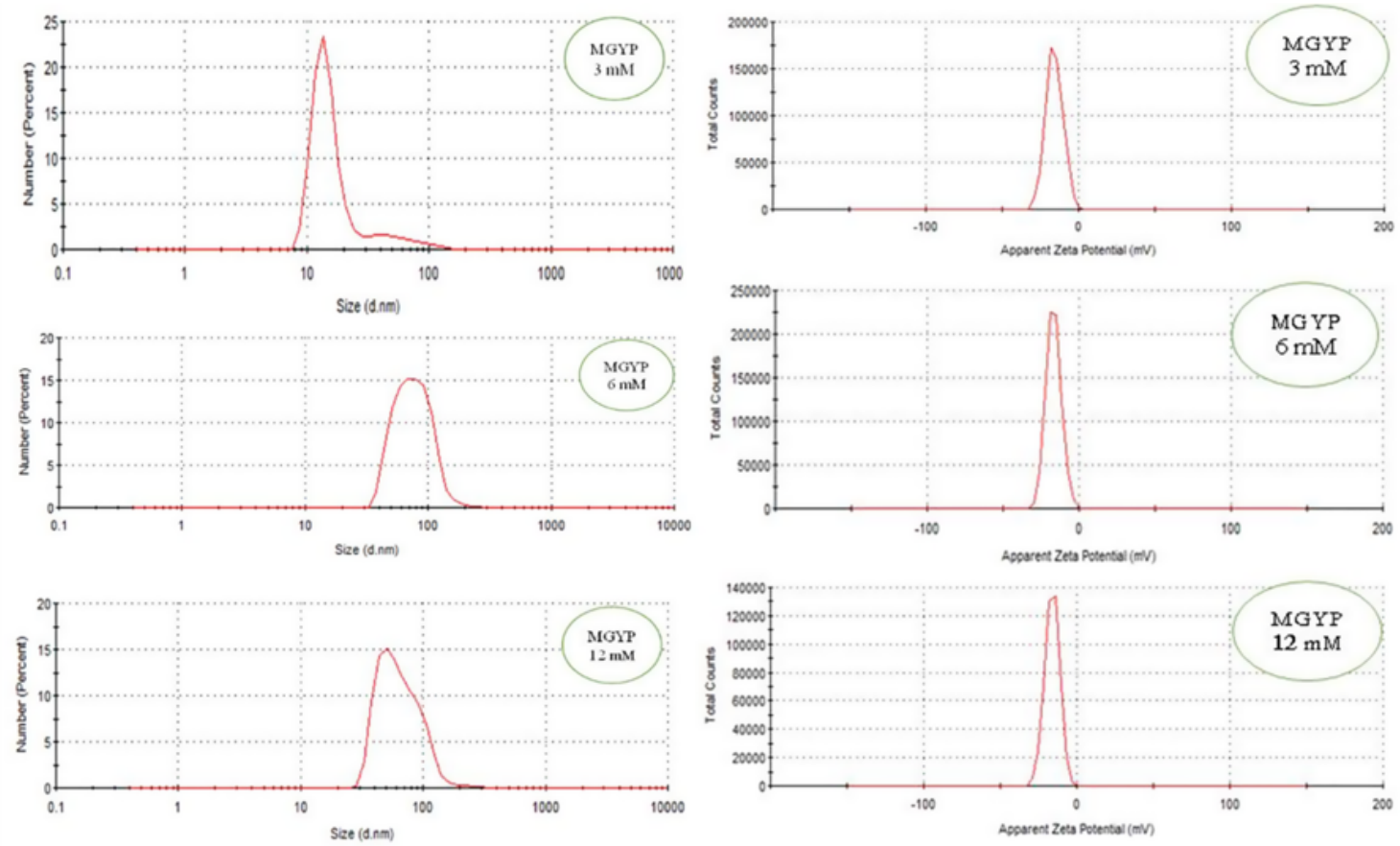

Figure 2

The size and the zeta potential of the biosynthesized AgNPs in three different concentrations of $AgNO_3$.

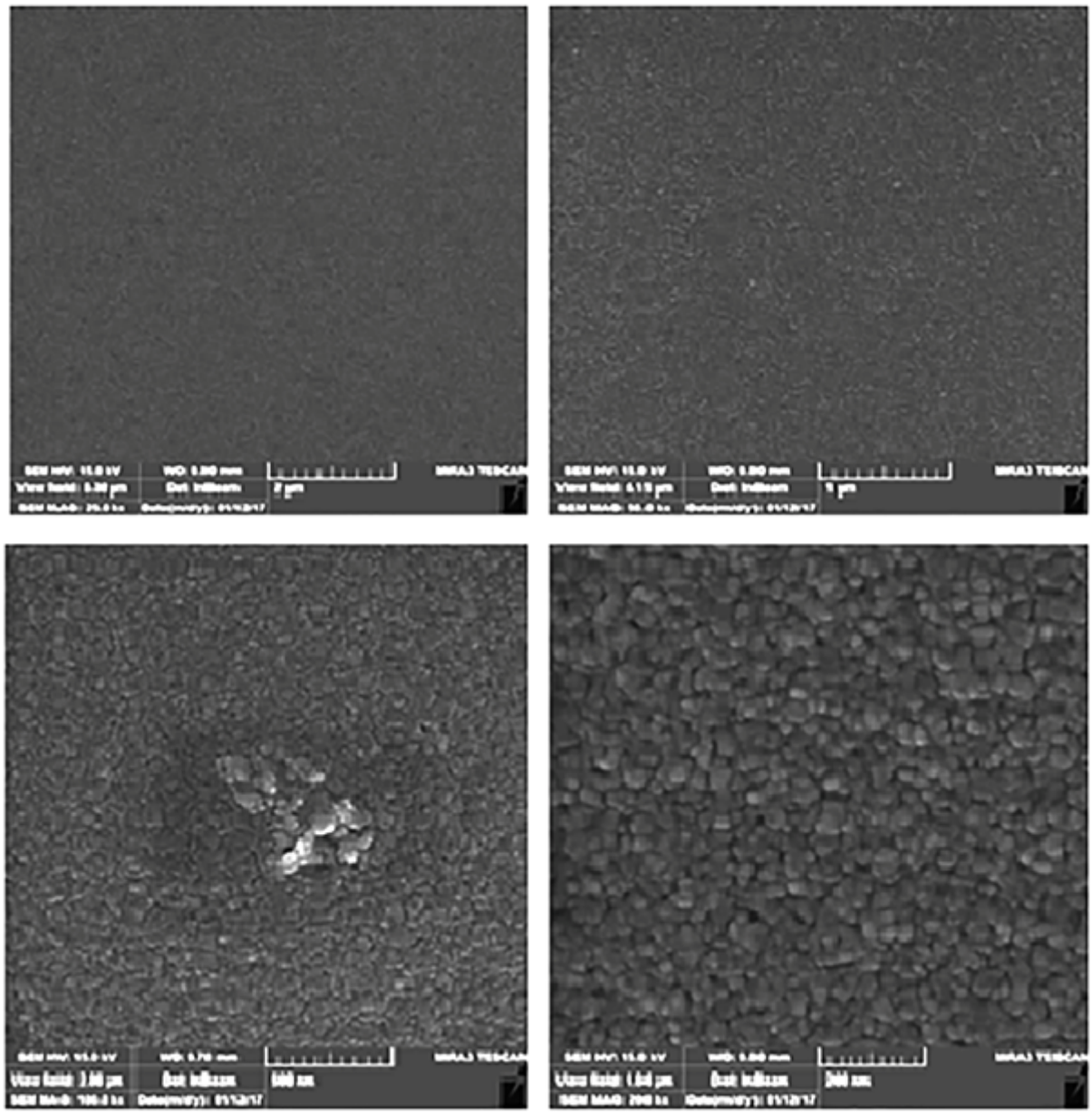

Figure 3

FE-SEM of biosynthesized AgNPs at 1, 2 µm, 500, and 200nm scale.

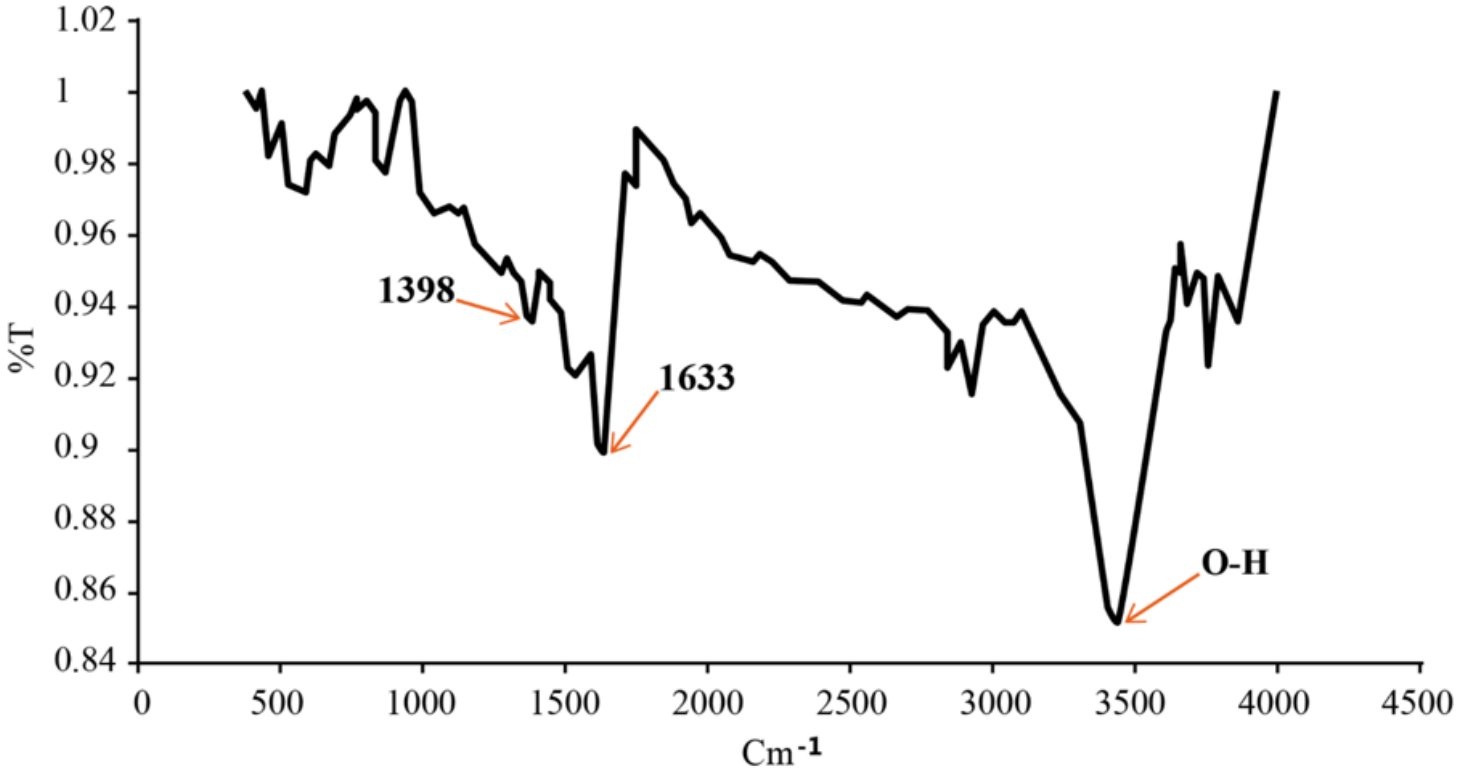

Figure 4

The FTIR analysis of biosynthesized AgNPs.

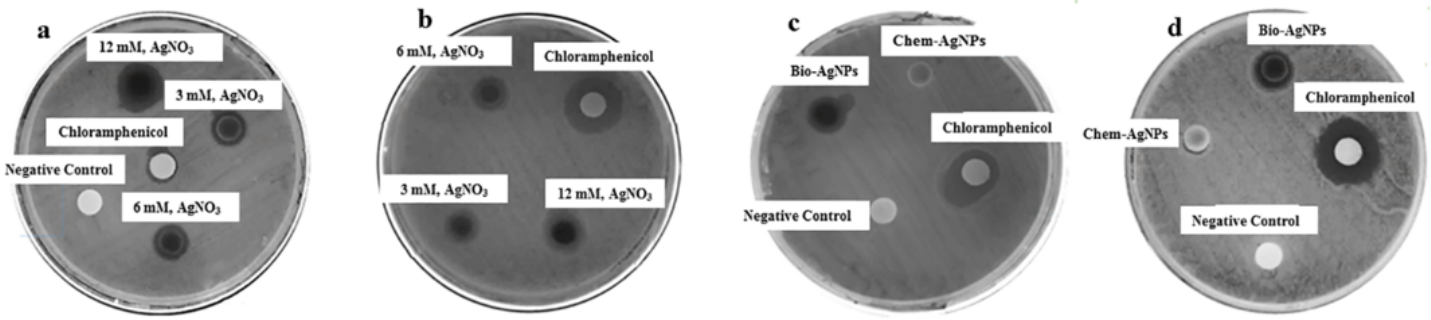

Figure 5

Disk diffusion method using *E. coli* (a) and *S. aureus* (b) for produced Bio-AgNPs at three concentrations of $AgNO_3$; comparison of the antibacterial activity of Bio-AgNPs and Chem-AgNPs against *E. coli* (c) and *S. aureus* (d).

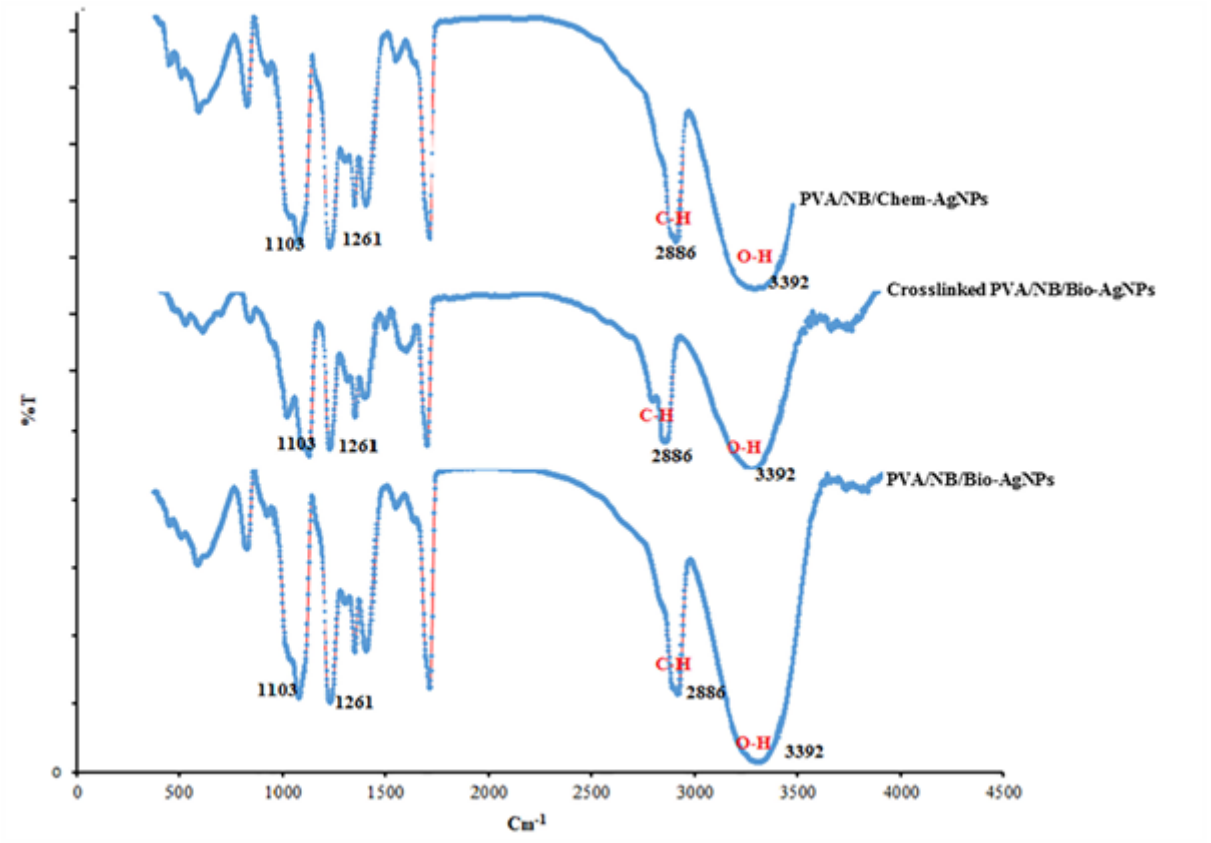

Figure 6

FTIR analysis of the produced PVA/NB/Chem-AgNPs, PVA/NB/Bio-AgNPs and crosslinked PVA/NB/Bio-AgNPs composite nanofiber.

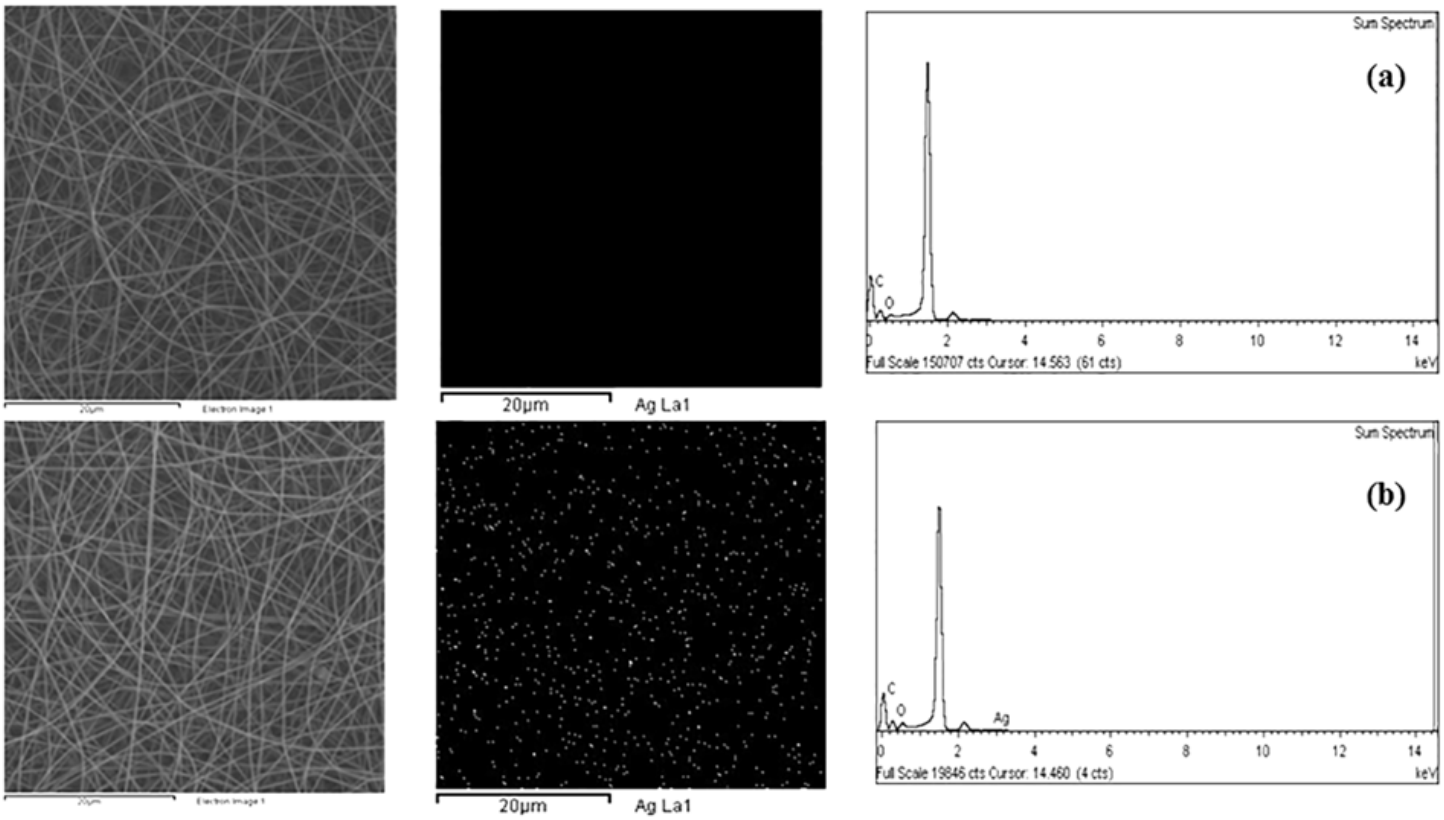

Figure 7

EDX of PVA/NB (a) and PVA/NB/Bio-AgNPs (b) composite nanofibers.

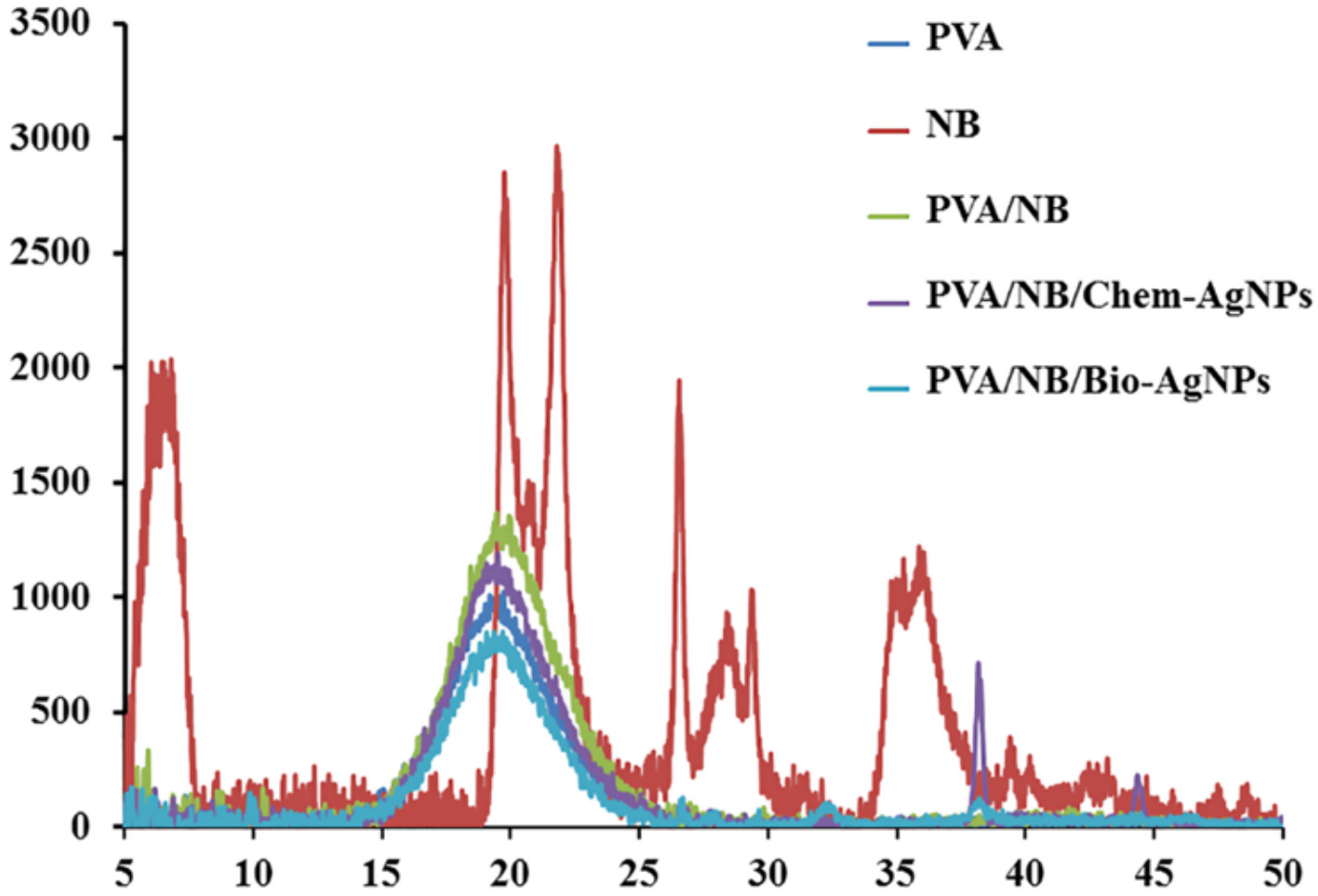

Figure 8

XRD results for NB, PVA, PVA/NB, PVA/NB/Bio-AgNPs, and PVA/NB/Chem-AgNPs.

Supplementary Files

This is a list of supplementary files associated with this preprint. Click to download.

- GA.tif